JOURNAL OF VIROLOGY, Dec. 1997, p. 9150–9156 Vol. 71, No. 12
0022-538X/97/$04.00+0

Rous Sarcoma Virus Direct Repeat *cis* Elements Exert Effects at Several Points in the Virus Life Cycle

SAMANTHA B. SIMPSON,[1] LEI ZHANG,[1]† REBECCA C. CRAVEN,[2] AND C. MARTIN STOLTZFUS[1]*

Department of Microbiology, University of Iowa, Iowa City, Iowa 52242,[1] and Department of Microbiology and Immunology, Pennsylvania State University College of Medicine, Hershey, Pennsylvania 17033[2]

Received 23 April 1997/Accepted 5 September 1997

Two ~135-nucleotide (nt) direct repeats flank the Rous sarcoma virus (RSV) oncogene *src* and are composed of two smaller repeats, dr1 (~100 nt) and dr2 (~36 nt). These sequences have been reported to contain *cis*-acting signals necessary for RNA packaging and elements that allow cytoplasmic accumulation of unspliced RNA (cytoplasmic transport elements). In this report, we show that avian fibroblasts infected with the Prague A strain of RSV with precise deletions of both dr1 elements express *src* and are transformed by this mutant virus but production of virus particles is very low and virus spread throughout the culture requires several weeks. We show that the replication defect is due to complex effects on viral RNA transport, viral RNA half-life, and virus particle assembly. The dr1 elements may contain binding sites for a permissive cell-specific factor(s) that facilitates efficient nuclear-cytoplasmic transport, RNA stability, and cytoplasmic utilization of unspliced viral RNA. The implications of these results for understanding the defects of nonpermissive virus infections in mammalian cells are discussed.

The genome of the Prague A strain of Rous sarcoma virus (RSV) contains two ~135-nucleotide (nt) imperfect direct repeat (DR) elements that flank the *src* gene (see Fig. 1). These repeats, which are approximately 80% homologous and predicted to form stem-loop structures, are composed of two smaller repeats, dr1 (~100 nt) and dr2 (~36 nt) (5). One of the repeats (upstream DR) is immediately downstream from the *env* gene, and the other (downstream DR) is downstream of the *src* gene in the 3′ untranslated region. In the case of the downstream DR, dr1 and dr2 are separated by an additional 52-nt element referred to as the E element. DR elements have been postulated to contain RNA packaging signals which are required in addition to the packaging signal in the 5′ leader sequence (24). More recently, fragments of the Prague C RSV genome containing the dr1 elements were shown to substitute for human immunodeficiency virus type 1 (HIV-1) Rev and the Rev-responsive element (RRE) in several HIV-1 expression constructs and facilitate cytoplasmic accumulation and expression of unspliced RNA in chicken embryo fibroblasts (CEF) (18). Several other simple primate retroviral genomes contain posttranscriptional regulatory elements in their 3′ untranslated regions which, when placed within the HIV-1 genome, complement the loss of either the RRE or the *trans*-acting HIV-encoded factor Rev and, when present, allow Rev-independent HIV replication (4, 33). Since Rev contains a nuclear export signal and facilitates transport of unspliced RRE-containing RNA from the nucleus to the cytoplasm (7–10, 14, 15, 33), these elements in the simple retroviruses which lack posttranscriptional regulatory proteins analogous to Rev have been termed constitutive transport elements (CTEs).

Consistent with a crucial role for the DR elements in virus replication, RSV mutants lacking dr1 elements have been shown not to replicate in avian cells (18, 24). These mutants were constructed by removal of large regions of the RSV genome which include the *src* gene and the region of the *src* 3′ splice site, as well as the dr1 sequences. To probe the function of the DR elements in the context of the intact RSV genome, we have analyzed an RSV mutant in which the two dr1 elements were precisely deleted. This virus mutant undergoes infections in permissive avian cells in which *src* is expressed but in which virus particle production is very low. Surprisingly, in addition to effects on the ratio of nuclear to cytoplasmic RNA, we found that the viral polyprotein Pr76^{gag} synthesized in these infected cells was not efficiently processed and mature viral proteins were not detected in extracellular virions.

MATERIALS AND METHODS

Plasmids. pJD100 is an infectious nonpermuted clone of a Prague A strain of RSV. pJTM14 was created by cloning the entire provirus derived from pJD100 into a pUC18-based vector containing the *cat* gene and the simian virus 40 early poly(A) signal (16). Nucleotide numbers are from the Prague C RSV sequence (22). Plasmid pSBS48 was constructed by annealing of the oligonucleotides 5′-CAGTTATAATAATCCTGCGAATCGGGCTGTAACGGGGC-3′ and 5′-TCGAGCCCCGTTACAGCCCGATTCGCAGGATTATTATAACTGAGCT-3′, followed by ligation to pJTM14, which was cleaved with *Sac*I and *Xho*I. This created a deletion between nt 6907 and nt 6983. pSBS48 was then cleaved with *Sac*I and the *Sac*I/*Sac*I fragment (nt 255 to nt 6865) from pJD100 was ligated to the cleaved plasmid to create pSBS50. Plasmid ΔUDR was then made by isolating the *Kpn*I/*Mlu*I fragment (nt 4995 to nt 7901) from pSBS50 and inserting it into pJD100, which was cleaved with *Kpn*I and *Mlu*I. Plasmid pSBS76 was created by a three-fragment ligation in which two PCR products were cloned between the *Bgl*II site at nt 7736 and the *Hin*dIII site at nt 9393. This created a deletion between nt 8796 and nt 8881. pSBS76 was then cleaved with *Mlu*I and *Hin*dIII, and the *Mlu*I/*Hin*dIII fragment (nt 7901 to the *Hin*dIII site in pBR322, which flanks the 3′ long terminal repeat) was ligated with the *Hin*dIII/*Cla*I fragment from pBR322 and the *Cla*I/*Mlu*I fragment from pJD100 to create ΔDDR. Plasmid ΔBDR was created by ligating the *Cla*I/*Mlu*I fragment containing the UDR deletion from ΔUDR with the *Mlu*I/*Cla*I fragment containing the DDR deletion from ΔDDR. Plasmids used to make templates for analysis of RSV and *lacZ* RNA have also been previously described (2, 13).

Cell culture and DNA transfections. Secondary CEF were cultured in SGM (Medium 199 [Bethesda Research Laboratories, Inc., Gaithersburg, Md.] supplemented with 10% [vol/vol] tryptose phosphate broth and 5% [vol/vol] calf serum). Secondary turkey embryo fibroblasts (TEF) were cultured in SGM supplemented with 1% (vol/vol) heat-inactivated chicken serum. CEF and TEF were transfected either by the DEAE-dextran procedure as previously described (16) or by the calcium phosphate coprecipitation procedure essentially as previously described (31).

* Corresponding author. Fax: (319) 335-9006. E-mail: marty-stoltzfus@uiowa.edu.

† Present address: Department of Laboratory Medicine, University of California, San Francisco, CA 94143.

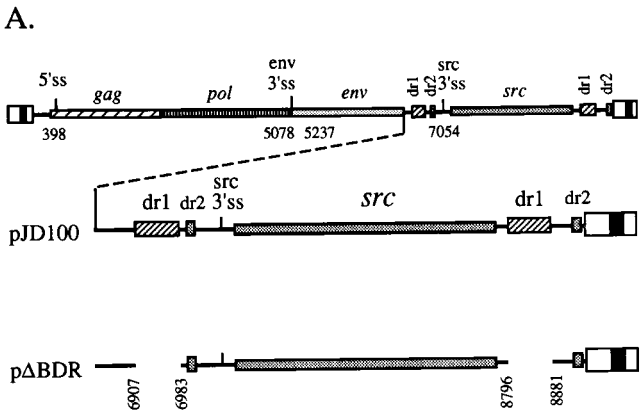

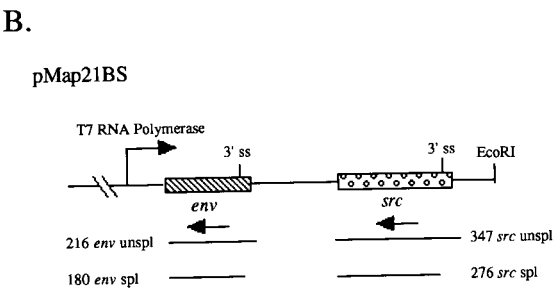

FIG. 1. Schematic representations of the Prague A RSV-proviral constructs and the riboprobe templates. (A) Diagrams of the wild-type RSV proviral DNA (pJD100) and mutant construct. Deletions are indicated by gaps in the constructs, with start and end points and other sites of interest marked by nucleotide number according to the Prague C RSV sequence (22). Abbreviations: 5′ss, 5′ splice donor; env 3′ss, *env* 3′ splice acceptor; src 3′ss, *src* 3′ splice acceptor; dr, direct repeat. (B) Riboprobe template used to analyze the RSV proviral RNA by RNase protection assays. Plasmid pMap21BS spans the *env* 3′ splice site (nt 5042 to 5258) and the *src* 3′ splice site (nt 6983 to 7330) with a heterologous sequence as a spacer. The plasmid was linearized with *Eco*RI, and antisense RNA was transcribed by using T7 RNA polymerase. The sizes of the fragments protected by each RNA species are indicated below the riboprobe maps.

RNA isolation and analysis. Total cellular RNA was harvested by the guanidine hydrochloride technique essentially as described by Strohman et al. (27). Cytoplasmic and nuclear RNAs were isolated as previously described (23). This preparation was followed by phase-contrast microscopic observation, and the purified nuclei appeared to be free of cytoplasmic tags. RNase protection analyses using [α-^{32}P]UTP-labeled riboprobes indicated that the nuclear but not the cytoplasmic RNA fraction contained unspliced c-*src* RNA precursors. RNase protection assays were carried out essentially as described previously (2).

Protein analysis. Cells were labeled with [^{35}S]methionine after starving in methionine-free medium (50 μCi/ml in Fig. 7 and 125 μCi/ml in Fig. 8). For the data shown in Fig. 7, cell monolayers were lysed as described previously, except that after disruption in radioimmunoprecipitation assay buffer, the lysates were centrifuged at full speed in a tabletop microcentrifuge for 10 min rather than in an ultracentrifuge (26). For the data shown in Fig. 7, the cell monolayers were lysed and immunoprecipitations were carried out as described previously (29).

RESULTS

Prague RSV dr1 deletion mutants transform avian cells but demonstrate delayed-replication phenotypes and a decrease in particle production. The effects of precisely deleting both dr1 elements in the context of the Prague A RSV genome (Fig. 1A) were tested by transfection of a mutant proviral DNA construct (ΔBDR) into either permissive CEF or TEF. Both cell types yielded similar results in the experiments described below. Under these conditions, the replication-competent phenotype can be determined by the ability of infectious virus to spread from the originally transfected cells, which represent only 5 to 10% of the cells, to the remainder of the nontransfected cells in the culture. To assay for the production of virus particles, reverse transcriptase (RTase) activity in the culture medium was measured at intervals after transfection (Fig. 2). RTase was detected in the wild type at 5 days after transfection, and its level was increased at 7 days. In contrast, RTase activity was not detected in the medium of ΔBDR-transfected cells, even at 28 days posttransfection. Despite the low levels of RTase, the majority of cells were morphologically transformed and expressed *src*, as shown by an immunofluorescence assay for the *src* protein pp60$^{v\text{-}src}$ (Fig. 3). Low levels of infectious virus could be detected by focus assays of the culture medium ($\sim 10^2$ focus-forming units/ml at 28 days compared to a wild-type level of $\sim 10^6$ focus-forming units/ml at 7 days), indicating virus spread.

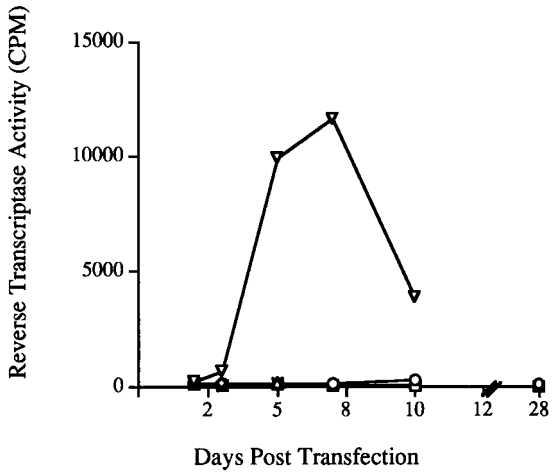

FIG. 2. Comparison of virus particle production by cells infected with wild-type RSV (▽) or a dr1 deletion mutant (○). After transfection of CEF with proviral DNA or control DNA (mock transfection [□]), culture medium was analyzed for RTase activity at the various posttransfection times indicated by using previously described techniques (32). The amount of [α-^{32}P]TTP-labeled product, which is proportional to the number of virions released from CEF over the time course of infection, is plotted. Cells were passaged as they became confluent, and the medium was changed 24 h prior to harvesting of the medium for analysis. Constructs are described in Fig. 1. Data shown is representative of several independent transfections in both CEF and TEF.

Cells infected with the dr1 deletion mutant express viral RNA. Since previous studies have indicated that RSV constructs lacking dr1 elements fail to replicate (18, 24) but our data showed low levels of virus infection, we carried out additional experiments to characterize this process. Total RNA was isolated from infected cells at various times after transfection, and the probe derived from pMap21BS shown in Fig. 1B was used to detect unspliced *gag-pol*, *env*, and *src* mRNAs by RNase protection assays (Fig. 4A). Viral RNA in the ΔBDR-infected cells was barely detectable at 10 days, but at 28 days, these cells contained significant levels of RNA corresponding to the three species of viral RNA. The RNA data, together with the *src* immunofluorescence and RTase assays, indicated that virus in which both dr1 elements were deleted was produced in very low amounts but after several weeks was able to spread throughout the cell culture. Examination of the viral RNA in ΔBDR-infected cells by reverse transcription-PCR indicated that the deletions of the dr1 elements were maintained after 28 days. Likewise, Northern blots indicated that there were no deletions in the unspliced, *env*, and *src* mRNA species compared to wild-type RNA, other than the expected minor changes in mobility arising from the dr1 deletions (data

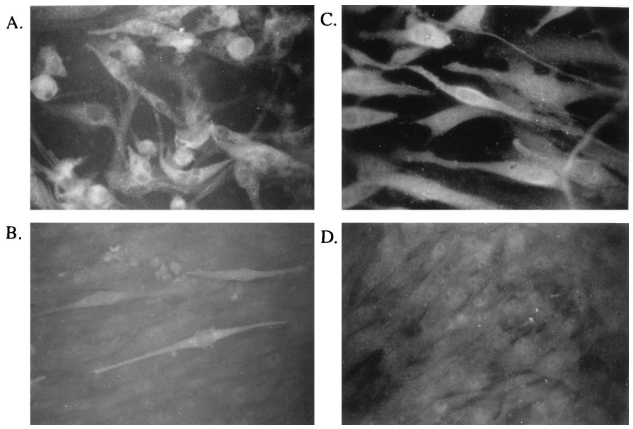

FIG. 3. Immunofluorescence detection of v-*src* in cells expressing the wild-type or the mutant virus with dr1 deleted. Cells were grown on glass coverslips and analyzed by immunofluorescence assay every 3 days posttransfection by using mouse v-*src* monoclonal antibody EC10 (19) as the primary antibody and a goat anti-mouse antibody conjugated with fluorescein isothiocyanate as the secondary antibody. EC10 reacts strongly with v-*src* and cross-reacts weakly with c-*src*. Photographs were taken with the 40× objective of a fluorescence microscope. (A) TEF infected with the wild type at 6 days posttransfection. (B) TEF infected with the dr1 deletion (ΔBDR) mutant at 9 days posttransfection. (C) TEF infected with the ΔBDR mutant at 24 days posttransfection. (D) TEF transfected with no DNA at 24 days posttransfection.

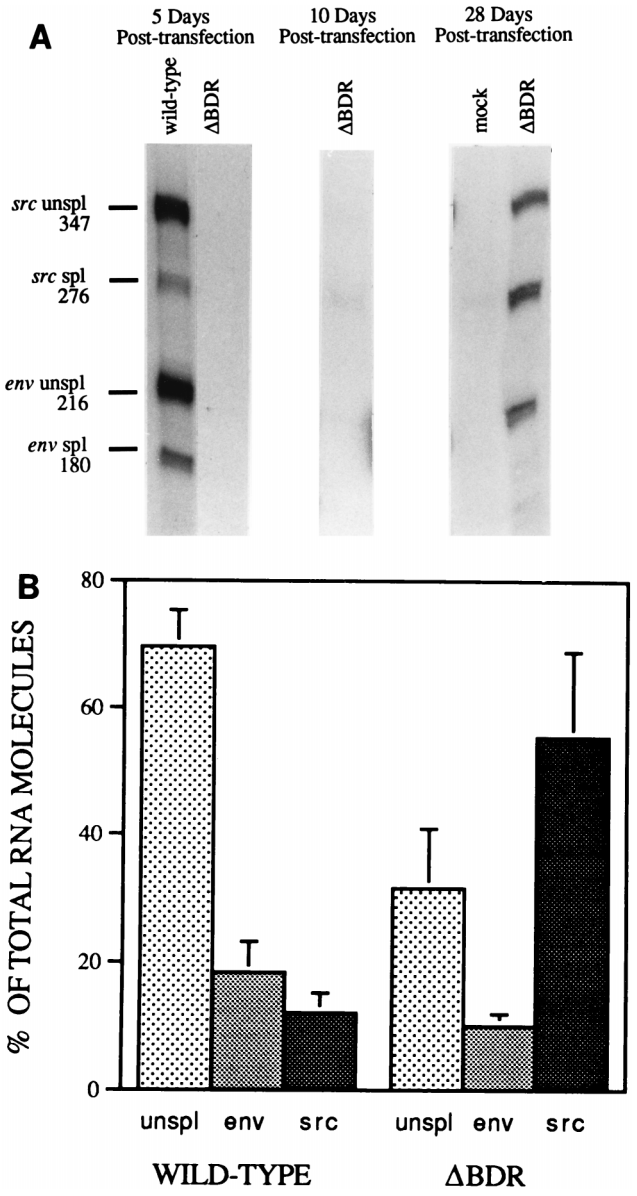

FIG. 4. Altered steady-state ratios of viral RNA species in CEF infected with dr1 deletion mutants. (A) RNase protection assays of total cell RNA isolated 5 days (5 μg), 10 days (5 μg), and 28 days (10 μg) posttransfection by using the pMap21BS riboprobe labeled with [^{32}P]UTP carried out as described in Materials and Methods. Wild-type and mutant constructs are described in Fig. 1. The sizes in nucleotides and locations of the protected bands are indicated. (B) Percentages of viral RNA molecules calculated from the amounts of radioactivity in the protected bands, as determined by direct counting of the gels with an AMBIS beta scanner. The amounts of radioactivity were then corrected for the number of uridine residues in the protected bands. The 276-nt spliced (spl) *src* band was used for total *src* mRNA, the 180-nt spliced *env* band was used for total *env* mRNA, and the 216-nt unspliced (unspl) *env* band was used for total unspliced mRNA. The value determined for each of these bands was divided by the sum total of the three bands and multiplied by 100 to give the percentage of RNA molecules. The 347-nt unspliced *src* band arises from protection by both unspliced and *env* mRNAs and was not used in these calculations. Similar results were obtained with TEF.

not shown). Virus from the medium of the mutant-infected cells was used to infect new CEF. These infected cells exhibited the same delay in transformation and absence of detectable RTase activity. These results suggested that the virus which spread in the ΔBDR-transfected cells was not revertant.

We also determined the relative amounts of different viral RNA species in cells infected with the mutant viruses. The data in Fig. 4B, based on multiple RNase protection experiments, indicated that the levels of both unspliced *gag-pol* mRNA and *env* mRNA were reduced in ΔBDR-infected cells relative to those in wild-type-infected cells. Concomitant with the decreases in *env* and unspliced *gag-pol* mRNAs, there was a corresponding increase in the level of *src* mRNA.

Unspliced *gag-pol* and *env* mRNAs are unstable in cells infected by mutants lacking dr1 elements. To determine whether the absence of the dr1 elements affected RNA stabilities and to what extent this correlated with the differences between the mutant and wild type in steady-state RNA levels, we performed analyses in which transcription was blocked at zero time with dactinomycin and infected cell cultures were harvested at 3-h intervals after treatment with the drug (Fig. 5A). Viral RNA was analyzed at each time point by RNase protection assays. The fraction of the RNA species remaining at each time point was measured by beta scanning, and the half-lives of all of the species were determined from the slopes of semilogarithmic plots of the data. The wild-type unspliced, *env*, and *src* mRNAs decayed with half-lives of 6, 16, and 11 h, respectively (Fig. 5B). This is in good agreement with our previously reported data on the stabilities of another RSV strain, B77 avian sarcoma virus (25). The results shown in Fig. 5B indicated that the decay of unspliced RNAs in ΔBDR-infected cells occurred significantly faster than that of unspliced RNA in wild-type-infected cells. The *env* mRNA also decayed more rapidly in ΔBDR-infected cells than in wild-type-infected cells. The decay rate of *src* mRNA was also increased by the dr1 deletions but to a lesser extent than that of the unspliced RNA and *env* mRNA. These results indicate that the reduction in the percentages of unspliced RNA and *env* mRNA in ΔBDR-infected cells (Fig. 4B) is correlated with a decrease in the half-life of these RNA species. There is a concomitant increase in the percentage of *src* mRNA, whose half-life is affected to a lesser extent.

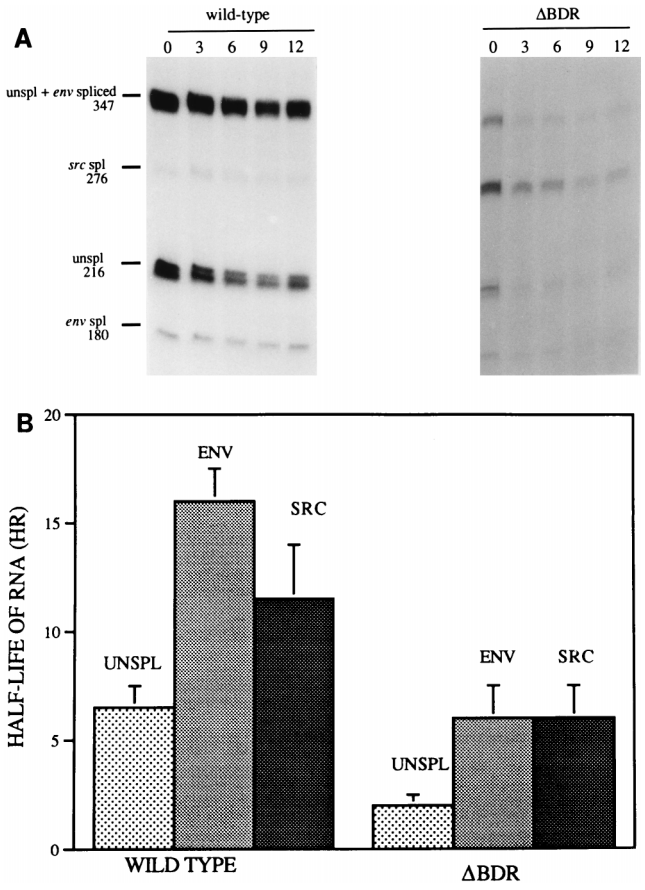

FIG. 5. Comparison of stabilities of viral mRNA species in cells infected with wild-type RSV and dr1 deletion mutant RSV constructs. (A) Infected-cell RNA harvested at various time points (indicated in hours) after the addition of dactinomycin (1 μg/ml). This concentration is sufficient to inhibit bulk cellular poly(A)$^+$ RNA by more than 95%. RNase protection assays using a pMap21BS riboprobe were performed, and the amounts of each RNA species were determined by direct counting of the gels on an AMBIS beta scanner as described in the legend to Fig. 4. unspl, unspliced. (B) Log of the fraction of RNA remaining for each species plotted versus time after dactinomycin addition. The half-lives were determined from the slope of the line, and these values are shown.

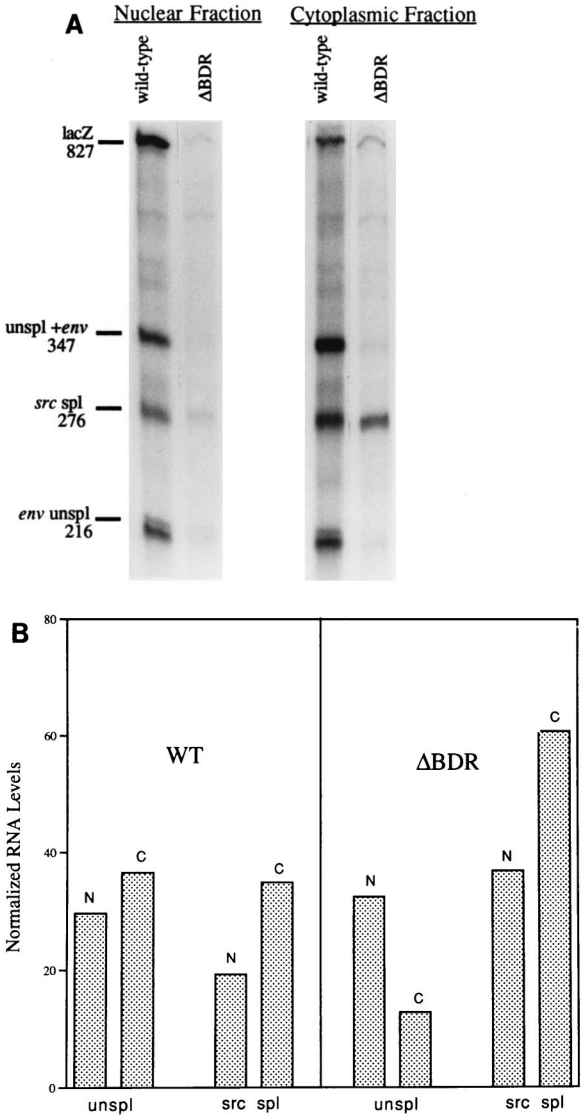

FIG. 6. Comparison of nuclear and cytoplasmic viral RNA levels in wild-type RSV and in the dr1 deletion mutant. (A) RNase protection assays of nuclear and cytoplasmic CEF RNAs (6 and 15 μg, respectively) harvested at 48 h after transfection of the wild type and the dr1 deletion mutant carried out with pMap21BS and pMapLacZ riboprobes. Plasmid pGAGLAC532BS, which produces an RSV *gag-lacZ* fusion mRNA, was used as a cotransfection control. spl, spliced; unspl, unspliced. (B) Amounts of unspliced *src* and LacZ RNA were determined by directly counting the gel on an AMBIS beta scanner, and RNA levels, determined as described in the legend to Fig. 4, were then normalized to the amount of *lacZ* RNA to determine the relative levels of nuclear (N) and cytoplasmic (C) unspliced RNAs and *src* mRNA. WT, wild type.

Mutant lacking dr1 elements demonstrates an elevated ratio of nuclear to cytoplasmic RNA. It has previously been shown that cells transfected with a Prague C RSV construct lacking dr1 sequences have a reduced level of unspliced viral RNA in the cytoplasm (18). To confirm this effect of the dr1 deletions on nuclear and cytoplasmic RNA levels for the Prague A ΔBDR mutant, cells were transiently transfected for 48 h with mutant and wild-type proviral DNA constructs. Preliminary studies indicated that spread of wild-type virus from the initially transfected cells occurred within this time period. Thus, to confine virus expression only to the initially transfected cells and to avoid this complication, we used constructs which contained several point mutations within the viral integrase gene. These mutations do not cause any changes in the stability or splicing ratios of RSV RNA but severely inhibit the ability of the virus to replicate (3, 11). Use of these nonreplicating virus constructs allowed valid comparisons of RNA levels in different transfections by including an internal control plasmid. As an internal control for these studies, we cotransfected plasmid pGAGLAC532BS, an RSV plasmid with an intact downstream DR sequence and the β-galactosidase reporter gene fused in frame with the *gag* gene (13). The nuclear and cytoplasmic fractions were prepared as described in Materials and Methods, and the levels of the various viral RNA species were quantitated by RNase protection assays. The results of a representative assay are shown in Fig. 6A. In this experiment, the transfection efficiency of the ΔBDR mutant was lower than that of the wild type, as indicated by the difference in the signal of the 827-nt *lacZ* protected fragment. As shown in Fig. 6B, the nuclear levels of unspliced RNA were similar in cells transfected with either the dr1 mutant or the wild-type genome RNA when normalized to the *lacZ* RNA signals. In contrast, the level of mutant cytoplasmic RNA was reduced. These results are in agreement with those of Ogert et

al., who reported a significantly reduced cytoplasmic-to-nuclear RNA ratio in cells transiently transfected with a Prague C RSV construct lacking dr1 elements (18). Figure 6B shows that the spliced *src* mRNA levels in both the nuclear and cytoplasmic fractions normalized for *lacZ* were elevated in the dr1 mutant but the ratio of nuclear to cytoplasmic *src* mRNA was similar to that of the wild type. Because of the lower signals of *env* mRNA in the nuclear fraction, we were not able to accurately determine the nuclear-cytoplasmic distribution of spliced *env* in these experiments.

Unspliced *gag-pol* mRNA is translated in cells infected with mutants lacking dr1 elements. Comparison of the data indicated that there was a significantly greater effect of the dr1 deletions on particle production, which was reduced greater than 99% (Fig. 2), compared to the effects on levels of cytoplasmic unspliced viral RNA, which were reduced approximately threefold in the transient transfection experiments shown in Fig. 6. To determine if there were significant differences in the levels of translation products of the unspliced *gag-pol* mRNA when the RNAs lacked dr1 elements, we determined the relative amounts of *gag* polyprotein precursor synthesized in infected cells. TEF infected with wild-type RSV and ΔBDR mutant RSV were pulse-labeled with [^{35}S]methionine for 30 min. Because the kinetics of virus spread differed between the mutant and the wild type, we used cells at 5 days posttransfection for the wild-type virus and at 21 days posttransfection for the ΔBDR virus. Cells were lysed and immunoprecipitated with antiserum to capsid (CA) protein. Immunoprecipitates were subjected to sodium dodecyl sulfate (SDS)-polyacrylamide gel electrophoresis (PAGE), and the results are shown in Fig. 7B. A major labeled band corresponding to the Gag precursor was present in each case. The amounts of Pr76^{gag} synthesized, as determined by densitometric analysis of the protein gel, were compared to the relative amounts of unspliced RNA isolated from parallel cell cultures determined by RNase protection analysis (Fig. 7A). These results (Fig. 7C) indicated that in this experiment there was an approximately 11-fold reduction in the amount of Pr76^{gag} synthesized in the cultures infected with the ΔBDR mutant, and this was concomitant with an approximately 5-fold decrease in the level of total unspliced RNA. The greater effect on the translation of unspliced RNA compared to the amount of total viral RNA almost certainly is a consequence of the reduced proportion of the unspliced mutant RNA which is present in the cytoplasm and available for translation (Fig. 6B).

The Gag protein of the ΔBDR mutant does not assemble or process. The effects of the dr1 deletions on cytoplasmic RNA accumulation and translation of Pr76^{gag} were too small to explain the greater than 99% reduction in particle production by the RTase activity in Fig. 2. Therefore, to test whether assembly and processing of Pr76^{gag} were affected by deletion of dr1 elements, we carried out a 20-min [^{35}S]methionine pulse, followed by 20-, 45-, and 195-min chase periods to determine the fate of the Gag precursor protein in the wild-type- and mutant-infected TEF. The appearance of labeled mature Gag protein in virus particles was also monitored. The results of the SDS-PAGE analysis are shown in Fig. 8A. The disappearance of the Pr76^{gag} precursor and the appearance of mature CA protein in the medium are plotted in Fig. 8B. After the pulse, most of the radioactive label appeared in the Pr76^{gag} band in both wild-type- and mutant-infected cells. During the chase in wild-type-infected cells, the Pr76^{gag} band decreased and increasing amounts of label appeared as processed CA protein in the infected-cell lysates. In the medium, the radioactive label appeared as CA in released virus and this increased with the chase time. In contrast, in the ΔBDR-infected cells, Pr76^{gag} was stable and remained almost entirely in the precursor form throughout the chase. Furthermore, little or no processed CA was detected in the ΔBDR-infected lysates or medium even when the autoradiogram shown in Fig. 8 was exposed for longer times. In addition to the virus-specific bands, several high-molecular-weight bands of host cell origin were present (marked with an asterisk in Fig. 8A) in all of the lysate and medium samples, including those from uninfected cells.

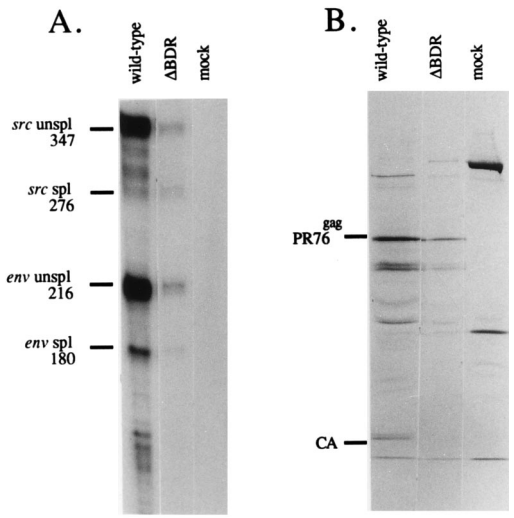

C.

	Unspliced RNA (CPM)	Amount of Pr76
wild-type	3625	587.8
ΔBDR	675	50.2

FIG. 7. Comparison of unspliced RNA and synthesis of Pr76^{gag} in TEF infected with the wild type and the dr1 deletion mutant. (A) RNase protection assay of total cellular RNA infected with wild-type (5 days posttransfection) and the ΔBDR mutant (21 days posttransfection) with a pMap21BS riboprobe were carried as described in Materials and Methods. spl, spliced; unspl, unspliced. (B) Immunoprecipitation of Pr76^{gag} with an antibody specific for the RSV CA protein. Infected cells were labeled for 30 min with [^{35}S]methionine, the cells were harvested, and immunoprecipitation of the cell lysates was carried out as described in Materials and Methods. Proteins were subjected to SDS–10% PAGE. (C) The amount of unspliced RNA was determined by directly counting the gel shown in panel A on an AMBIS beta scanner. The amount of Pr76^{gag} protein was determined by scanning densitometry of the gel in panel B. Prior to harvesting of the cells for RNA and labeling of the cells with [^{35}S]methionine, a single culture for each infection was split into two parallel 100-mm-diameter plates, which were used for the two assays.

The results of Fig. 8 indicated that the presence of dr1 elements in unspliced *gag-pol* mRNA is necessary for the Gag precursor to undergo efficient assembly and processing to mature protein products. The lack of Gag precursor processing in the mutant-infected cells is most likely a secondary result of the failure to assemble, since RSV *gag* mutants that fail to assemble also fail to process (30).

DISCUSSION

In this study, we have shown that an RSV mutant with precise deletions of both dr1 elements infects permissive avian fibroblasts but is severely impaired in the ability to replicate. This replication defect arises from activities of the dr1 elements that act at several points in the virus replication cycle. Our results are in agreement with previous studies showing that replication of RSV dr1 mutants is undetectable by release of RTase. However, in these earlier studies, the RSV genome

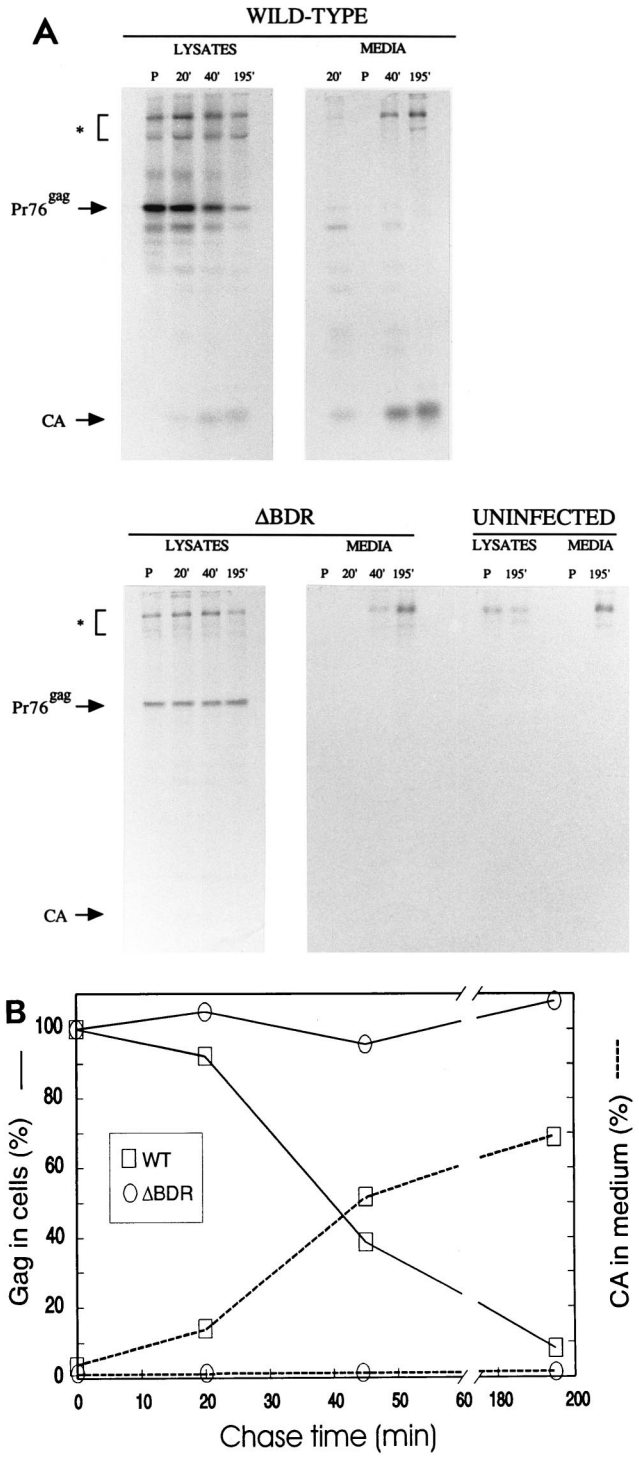

FIG. 8. Pulse-chase analysis of viral proteins in dr1 deletion mutant- and wild-type-infected cells. (A) TEF cell cultures infected with the wild-type or mutant virus labeled with [^{35}S]methionine in methionine-free medium for 20 min. After this time, the media and lysates were prepared from one set of 60-mm-diameter plates. The labeling medium was removed from duplicate sets of plates and replaced with medium containing normal amounts of methionine. The incubation was continued for 20-, 45-, and 195-min labeling periods, and the media and lysates were prepared from these cells. Gag proteins were immunoprecipitated with anti-RSV serum from both the media and lysates, and the immunoprecipitates were subjected to SDS–12% PAGE, followed by fluorography to detect the protein bands. The positions of Pr76^{gag} and CA are marked. The asterisk indicates the position of the high-molecular-weight host cell proteins present in the immunoprecipitates. We believe that bands may represent fibronectin protein which is secreted by the cells and is known to bind to the *Staphylococcus aureus* cells used in the immunoprecipitation procedure (21). P, pulse. (B) Amounts of Pr76^{gag} in the lysates (relative to the amount after the pulse) determined by PhosphorImager analysis of the gel and plotted versus chase time. The amounts of CA appearing in the medium relative to the amount of label in the pulse were determined by PhosphorImager analysis, and these values are plotted versus chase time. WT, wild type.

lacked the region of the genome containing the *src* gene and analysis of virus-infected cells was terminated at 10 days (18) and 7 days (24) postinfection. In our study, analysis of *src* expression by transformation and immunofluorescence and assays for the three different RSV RNA species were used to detect the low-level replication phenotype of the virus mutant.

First, in cells infected with the dr1 deletion mutant, the relative amount of viral RNA represented by spliced *src* mRNA is significantly elevated relative to those of unspliced *gag-pol* and *env* mRNAs. At least part of this difference from the wild-type pattern is due to the instability of both the unspliced and *env* mRNAs relative to the *src* mRNA. It is also possible that increased splicing at the *src* 3′ splice site contributes to the imbalance. Second, the ratio of cytoplasmic to nuclear unspliced viral RNA is lower in cells transfected with the mutant than in those infected with the wild type, suggesting that the dr1 element is able to facilitate the transport and/or the cytoplasmic stability of unspliced viral RNA. This is consistent with previous data showing that the dr1 sequence facilitates Rev-independent expression of unspliced RNA in avian cells when substituted in HIV constructs for the RRE sequence; i.e., dr1 contains sequences with the property of a CTE (18, 23a). Our results shown above clearly indicate, however, that the dr1 elements are not absolutely required for the transport and translation of unspliced RSV *gag-pol* mRNA.

Third, we found that in mutant-infected cells the *gag* precursor Pr76^{gag} is synthesized at levels consistent with the amount of unspliced viral RNA in the cytoplasm. Unexpectedly, however, the protein is not assembled into particles or processed into mature Gag proteins. These results differ from those of Ogert et al., who did not detect significant levels of intracellular Gag proteins in cells transiently transfected with a Prague C RSV mutant with the *src* gene and dr1 elements deleted (18). Whether this is due to differences in the viral strain or in the methods of detection (e.g., transfection versus infection) is not clear.

A previous study on Schmidt-Ruppin RSV concluded that the DR elements contain essential *cis*-acting RNA packaging signals in addition to the major Ψ packaging signal in the 5′ untranslated region (24). We have compared the effects of Ψ mutations and a dr1 deletion mutant on packaging by exploiting a previously described assay (13). These results indicated that whereas the Ψ mutations reduced specific RNA packaging 25-fold, the dr1 deletion reduced packaging less than 2-fold (32a). Thus, our data and that of others indicate that the effects of the dr1 on RNA transport, RNA stability, and particle assembly are more significant than the effect on packaging, at least in the context of the Prague RSV.

The effect of the dr1 deletions on virus particle assembly is most surprising since evidence to date has indicated that the assembly and release of retrovirus-like particles is a function of the Gag protein and that no other viral proteins are required (for a review, see reference 6). The *gag* sequences remain wild type in the mutant, and yet particle release is nearly abolished. We suggest two possible hypotheses. First, there may be a threshold level of Pr76^{gag} precursors necessary in the cell for efficient virus assembly to occur. The reduced level of un-

spliced RNA in the cytoplasm of cells infected with the dr1 deletion mutant may not allow sufficient translation of Gag for this threshold level to be reached. A second hypothesis is that dr1 may contain, in addition to the signal facilitating nuclear-cytoplasmic transport, a *cis* signal that localizes the unspliced RNA to particular places within the cell. *cis*-acting signals that target mRNAs to particular sites have been shown to be present in the 3′ untranslated regions of a number of cellular mRNAs in both somatic and germ cells (12). It is possible that such targeting is necessary for the translation products of the viral unspliced RNA to be assembled efficiently.

The nonpermissiveness of mammalian cells to wild-type RSV infections may result in part from the failure of the dr1 element to express its activities in these cells. A preponderance of *src* mRNA, the failure to cleave $Pr76^{gag}$, and a deficiency in nuclear-to-cytoplasmic RNA transport have all been reported to be properties of mammalian cells transfected or transformed by RSV (1, 17, 20, 28). These results suggest that mammalian cells may lack the factor(s) that interacts with the dr1 sequences. Consistent with this hypothesis, we have shown that, in the context of the HIV reporter constructs, dr1 substitutes for HIV Rev and the HIV RRE to facilitate expression of unspliced RNA in permissive avian cells but fails to substitute for HIV Rev and the HIV RRE in HeLa cells and human foreskin fibroblasts, suggesting a host cell dependence for the CTE activity of the element (23a).

ACKNOWLEDGMENTS

This research was supported by Public Health Service grants CA28051 to C.M.S. and CA 47482 to John Wills, in whose laboratory a portion of this work was performed.

We thank Stanley Perlman and Mark Stinski for critical reviews of the manuscript.

REFERENCES

1. **Berberich, S. L., M. Macias, L. Zhang, L. P. Turek, and C. M. Stoltzfus.** 1990. Comparison of Rous sarcoma virus RNA processing in chicken and mouse fibroblasts: evidence for double-spliced RNA in nonpermissive mouse cells. J. Virol. **64:**4313–4320.
2. **Berberich, S. L., and C. M. Stoltzfus.** 1991. Analysis of spliced and unspliced Rous sarcoma virus RNAs early and late after infection of chicken embryo fibroblasts: effect of cell culture conditions. Virology **182:**135–144.
3. **Berberich, S. L., and C. M. Stoltzfus.** 1991. Mutations in the regions of the Rous sarcoma virus 3′ splice sites: implications for regulation of alternative splicing. J. Virol. **65:**2640–2646.
4. **Bray, M., S. Prasad, J. W. Dubay, E. Hunter, K.-T. Jeang, D. Rekosh, and M.-L. Hammarskjold.** 1994. A small element from Mason-Pfizer monkey virus genome makes human immunodeficiency virus type 1 expression and replication Rev-independent. Proc. Natl. Acad. Sci. USA **91:**1256–1260.
5. **Coffin, J. M.** 1984. Structure of the retroviral genome, p. 261–368. *In* R. Weiss, N. Teich, H. Varmus, and J. Coffin (ed.), RNA tumor viruses, vol. 1. Cold Spring Harbor Laboratory, Cold Spring Harbor, N.Y.
6. **Craven, R. C., and L. J. Parent.** 1996. Dynamic interactions of the Gag polyprotein. Curr. Top. Microbiol. Immunol. **214:**65–94.
7. **Emerman, M., R. Vazeus, and K. Peden.** 1989. The *rev* gene product of the human immunodeficiency virus affects envelope-specific RNA localization. Cell **57:**1155–1165.
8. **Felber, B. K., M. Hadzopoulou-Cladaras, C. Cladaras, T. Copeland, and G. N. Pavlakis.** 1989. Rev protein of human immunodeficiency virus type 1 affects the stability and transport of the viral mRNA. Proc. Natl. Acad. Sci. USA **86:**1495–1499.
9. **Fischer, U., J. Huber, W. C. Boelens, I. W. Mattaj, and R. Luhrmann.** 1995. The HIV-1 Rev activation domain is a nuclear export signal that accesses an export pathway used by specific cellular RNAs. Cell **82:**475–483.
10. **Fischer, U., S. Meyer, M. Teufel, C. Heckel, R. Luhrmann, and G. Rautmann.** 1994. Evidence that HIV-1 Rev directly promotes the nuclear export of unspliced RNA. EMBO J. **13:**4105–4112.
11. **Horton, R., S. R. Mumm, and D. P. Grandgenett.** 1991. Phosphorylation of the avian retrovirus integration protein and proteolytic processing of its carboxyl terminus. J. Virol. **65:**1141–1148.
12. **Johnston, D. S.** 1995. The intracellular localization of messenger RNAs. Cell **81:**161–170.
13. **Knight, J. B., Z. H. Si, and C. M. Stoltzfus.** 1994. A base-paired structure in the avian sarcoma virus 5′ leader is required for efficient encapsidation of RNA. J. Virol. **68:**4493–4502.
14. **Lawrence, J., A. Cochrane, C. Johnson, A. Perkins, and C. Rosen.** 1991. The HIV-1 Rev protein: a model system for coupled RNA transport and translation. New Biol. **3:**1220–1232.
15. **Malim, M. H., J. Hauber, S.-Y. Le, J. V. Maizel, and B. R. Cullen.** 1989. The HIV-1 *rev trans*-activator acts through a structured target sequence to activate nuclear export of unspliced viral mRNA. Nature **338:**254–257.
16. **Miller, J. T., and C. M. Stoltzfus.** 1992. Two distant upstream regions containing *cis*-acting signals regulating splicing facilitate 3′-end processing of avian sarcoma virus RNA. J. Virol. **66:**4242–4251.
17. **Nasioulas, G., S. Hughes, B. K. Felber, and J. W. Whitcomb.** 1995. Production of avian leukosis virus particles in mammalian cells can be mediated by the interaction of the human immunodeficiency virus protein Rev and the Rev-responsive element. Proc. Natl. Acad. Sci. USA **92:**11940–11944.
18. **Ogert, R. A., L. H. Lee, and K. L. Beemon.** 1996. Avian retroviral RNA element promotes unspliced RNA accumulation in the cytoplasm. J. Virol. **70:**3834–3843.
19. **Parsons, S. J., D. J. McCarley, C. M. Ely, D. C. Benjamin, and J. T. Parsons.** 1984. Monoclonal antibodies to Rous sarcoma virus $pp60^{src}$ react with enzymatically active cellular $pp60^{src}$ of avian and mammalian origin. J. Virol. **51:**272–282.
20. **Quintrell, N., S. H. Hughes, H. E. Varmus, and J. M. Bishop.** 1980. The structure of viral RNAs in mammalian cells infected with avian sarcoma virus. J. Mol. Biol. **143:**363–393.
21. **Ryden, C., K. Rubin, P. Speziale, M. Hook, M. Lindberg, and T. Wadstrom.** 1982. Fibronectin receptors from *Staphylococcus aureus*. J. Biol. Chem. **258:**3396–3401.
22. **Schwartz, D. E., R. Tizard, and W. Gilbert.** 1983. Nucleotide sequence of Rous sarcoma virus. Cell **32:**853–869.
23. **Simpson, S., and C. M. Stoltzfus.** 1994. Frameshift mutations in the v-*src* gene of avian sarcoma virus act in *cis* to specifically reduce v-*src* mRNA levels. Mol. Cell. Biol. **14:**1835–1844.

23a. **Simpson, S., and C. M. Stoltzfus.** Unpublished data.

24. **Sorge, J., W. Ricci, and S. H. Hughes.** 1983. *cis*-acting RNA packaging locus in the 115-nucleotide direct repeat of Rous sarcoma virus. J. Virol. **48:**667–675.
25. **Stoltzfus, C. M., K. Dimock, S. Horikami, and T. A. Ficht.** 1983. Stabilities of avian sarcoma virus RNAs; comparison of subgenomic and genomic species with cellular mRNAs. J. Gen. Virol. **64:**2191–2202.
26. **Stoltzfus, C. M., S. K. Lorenzen, and S. L. Berberich.** 1987. Noncoding region between the *env* and *src* genes of Rous sarcoma virus influences splicing efficiency at the *src* gene 3′ splice site. J. Virol. **61:**177–184.
27. **Strohman, R., P. Moss, J. Micou-Eastwood, D. Spector, A. Przybyla, and B. Peterson.** 1977. Messenger RNA for myosin polypeptides: isolation from single myogenic cell cultures. Cell **10:**265–273.
28. **Vogt, V. M., D. A. Bruckenstein, and A. P. Bell.** 1982. Avian sarcoma virus *gag* precursor polypeptide is not processed in mammalian cells. J. Virol. **44:**725–730.
29. **Wills, J. W., R. C. Craven, and J. A. Achacoso.** 1989. Creation and expression of myristylated forms of Rous sarcoma virus *gag* protein in mammalian cells. J. Virol. **63:**4331–4343.
30. **Wills, J. W., R. C. Craven, R. A. Weldon, T. D. Nelle, and C. R. Erdie.** 1991. Suppression of retroviral MA deletions by the amino-terminal membrane-binding domain of $p60^{src}$. J. Virol. **65:**3804–3812.
31. **Zhang, L., S. B. Simpson, and C. M. Stoltzfus.** 1996. Selection and characterization of replication-competent revertants of a Rous sarcoma virus *src* gene oversplicing mutant. J. Virol. **70:**3636–3644.
32. **Zhang, L., and C. M. Stoltzfus.** 1995. A suboptimal *src* 3′ splice site is necessary for efficient replication of Rous sarcoma virus. Virology **206:**1099–1107.

32a. **Zhang, L., and C. M. Stoltzfus.** Unpublished data.

33. **Zolotukhin, A. S., A. Valentin, G. N. Pavlakis, and B. K. Felber.** 1994. Continuous propagation of RRE(−) and Rev(−)RRE(−) human immunodeficiency virus type 1 molecular clones containing a *cis*-acting element of simian retrovirus type 1 in human peripheral blood lymphocytes. J. Virol. **68:**7944–7952.